IJEMD-BMCR, (3) 2 (2025) https://doi.org/ 10.54938/ijemdbmcr.2025.03.1.438

International Journal of Emerging Multidisciplinaries:
Biomedical and Clinical Research

Research Paper
Journal Homepage: www.ojs.ijemd.com
ISSN (print): 2957-8620 ISSN (online): 2960-0731

Fabrication of Graphene-Based Tin Oxide (Sno_2) Composite With Improved Visible Light For The Photocatalytic Degradation of Methylene Blue

Williams Uyo Queen [1*], Tensaba Andes Akafa [2] , Abatyough Terungwa Michael [1] , Adewunmi Olufemi Oluwole [1]

1. Faculty of Science and Technology, Department of Chemical Sciences, Bingham University, Kuru, Nasarawa State, Nigeria
2. Faculty of Clinical Sciences, College of Health Sciences, Federal University Wukari, Taraba State, Nigeria

ABSTRACT

The SnO_2 nanoparticles were synthesized via the co-precipitation method by varying weight percentages (1%, 2%, 3% and 4%) of GO loaded on the SnO_2 nanoparticles. The effect of varied composition of GO on the SnO_2/GO nanocomposite were investigated using spectroscopic instruments such as Scanning Electron Microscope (SEM), Transmission electron microscope (TEM), X-ray diffraction (XRD), Element mapping, Energy Dispersive X-Ray Spectroscopy (EDX), the Fourier transform infrared spectroscopy (FT-IR), Brunauer-Emmett-Teller (BET), photoluminescence (PL), the Ultraviolet–visible spectroscopy (UV-Vis) and Diffuse reflectance spectrum (DRS) showed the successful formation of GO/SnO_2 nanostructures. furthermore, the photocatalytic activity of the GO/SnO_2 nanocomposites and SnO_2 were studied through the photodegradation of methylene blue under visible light irradiation. The degradation efficiencies of the GO/SnO_2 were much higher than that of pure SnO_2. From the results obtained, we believe that this current work will provide relevant views for further fabrication of other novel nanostructures and exploration of their applications.

Keywords : SnO2, Graphene Oxide, Nanocomposites, Photocatalysis, Methylene Blue

Email Address : ujah.william@binghamuni.edu.ng (**Williams Uyo Queen**)

INTRODUCTION

The usage of dyes as coloring agents in textile, paper, cosmetics, pharmaceutical, leather and food industries has attracted much attention over the years [1],[2]. This can be as a result of certain effects such as the contamination of water which mostly results from the textile industry and the consequences of these is attributed to the fact that dye molecules are difficult to remove, majority of these colored dyes are of synthetic origin and usually consist of aromatic rings in their molecular structure, Inert and non-biodegradable when discharged into wastewater without proper treatment [3],[4]. Therefore, removal of such dyes from wastewater requires urgency in a bid to protect human health and environmental resources. Methylene blue (MB), one of the most commonly used base dye, is considered to have multiple uses in the printing and dyeing industry [5]. In spite of the importance of MB in many industries, its presence in the environment can be bridged if not managed effectively [6]. MB is carcinogenic and does not degrade easily due to the characteristic stability of the aromatic rings in its molecular structure [3].

Traditional biological, chemical and physical techniques such as adsorption and chemical precipitation are recognized for the treatment of wastewater from dyeing industries [7]. These methods are expensive, form sludge or generate secondary pollutants, such as dye adsorption on activated carbon, where the pollutant is only converted from the liquid phase to the solid phase, causing pollution. Therefore, the decomposition of dyes into non-toxic compounds is essential and recommended [8]. The Advanced oxidation processes (AOP) are presently attracting a great deal of consideration in the field of water treatment [9]. These processes involve the use of mixture of photocatalysts composed of semiconductor heterojunctions [10]. Photocatalyst semiconductors such as tin dioxide (SnO_2) has attracted research interest recently, this is due to its high chemical stability, anti-photo-corrosion, powerful oxidation strength, non-toxicity, low cost, and outstanding catalytic performance [11].

However, the application of SnO_2 for the photodegradation of organic pollutants in aqueous matrices suffers from quick recombination of photogenerated electron-hole pairs, small surface area and the low solar energy conversion efficiency [12] owing to its large band gap of 3.6 eV. Hence, SnO_2 absorbs only UV light but visible light inactive [11]. This study, therefore, focuses on fabricating a novel photocatalyst that is capable of harnessing these limitations by modifying the structure of SnO_2 through doping with graphene oxide (GO) [12],[13] as well as the photocatalytic behaviors of the photocatalysts. The doping of semiconductors with Graphene Oxide (GO) is considered to be an attractive method as GO has the ability to drive charge separation efficiently, extend the lifetime of the charge carriers, and enhance the efficiency of the interfacial charge transfer to adsorbed dyes [14] due to its exceptional electrical conductivity and extremely efficient adsorption. Graphene oxide is a two-dimensional material with sp^2 bonded carbon atoms arranged in a honeycomb lattice known for its supportive nature in photocatalytic application due to its extraordinary advantages, such as large surface area superior electronic and excellent chemical stability [15].

REAGENTS AND MATERIALS

Graphene oxide, Stannous Chloride di-hydrate (98%), ammonia solution (25%), hydrochloric acid (37%), ethanol, methanol, and methylene blue (MB) were all purchased from Sigma Aldrich South Africa. Deionized water was used throughout this experiment. All chemicals used for this study were of analytical grade and used as received.

Preparation Of Tin-Oxide Sno_2 Nanoparticles

SnO_2 was prepared using the liquid phase co-precipitation method. About 2.00 g of Stannous chloride di-hydrate ($SnCl_2.2H_2O$) was dissolved in 100 ml deionized water in a beaker after which ammonia solution (25%) was added drop wise with constant stirring. The resulting gel-type precipitate form was filtered off and dried at 80 ^oC for 24 hr to remove water molecules. Finally, tin oxide nano-products was obtained through calcination at 550 ^oC for 4-6 hr.

Preparation Of Graphene Oxide-Tin Oxide (Go-Sno2) Nanocomposite

About 1.00 g of the prepared SnO_2 nanoparticles was dispersed in a beaker containing 120 ml of distilled water and ultrasonicated for 45 min at room temperature. The sonicated SnO_2 suspension was stirred continuously at room temperature for 45 min followed by the addition of different masses of GO (10,20,30,50 mg) to different aliquots to achieve equivalent weight percentages of 1,2,3 and 4 respectively. The resulting homogeneous mixtures was stirred, afterwards, 3 ml of HCl was added to each of them. The resulting suspensions was stirred again for another 45 min and then transferred into a 100ml Teflon-lined stainless autoclaves and kept at 180^oC in an oven and allowed to cool to room temperature. The resulting precipitates of the different doped amounts of GO nanocomposites was obtained via centrifugation and thereafter, washed severally with deionized water and ethanol. It was dried overnight in a hot air oven at 80^oC to obtain GO-SnO_2 nanocomposites which was grinded into GO-SnO_2 nano-powder.

Evaluation Of The Photocatalytic Activity

The photocatalytic ability of the photocatalysts were measured by the degradation rate of methylene blue (MB) under visible light. 50 mg of the synthesized SnO_2 as well as the various weight percentages of GO/SnO_2 (1%, 2%, 3% and 4%) was generally dissolved in 100 ml of MB aqueous solution (10 mg/L) at room temperature. Before irradiation, the solution was stirred well under dark conditions for 30 min to attain adsorption/desorption equilibrium. 5 mL of solution was taken every 20 min for analysis under a UV-visible spectrometer for 180 min. The visible light used in this test was replaced by a xenon lamp of 10 W capacity. The degradation efficiency of MB was determined using the equation given below:

Photodegradation efficiency (%) = [(C0 - Ct) / C0] = 100% -----(1)

where C0 is the initial concentration of MB, Ct is the concentration of MB at time, t.

Characterization

The X-ray diffraction pattern of the prepared nanocomposites were obtained using a Shimadzu 6100 X-ray diffractometer with a CU Kα radiation source (Bruker D6). The UV–Vis diffuse reflectance spectra (DRS) of the synthesized SnO_2/GO composites were measured with Pelkin-Elmer UV–Vis spectrophotometer, the photoluminescence (PL) emissions were obtained via Perkin Elmer LS 55 spectrofluorometer. The BET analysis (Micrometrics Tristar 3000) of the synthesized composites were carried out to determine their specific surface areas and their textural characteristics Their surface morphologies were also determined using the Scanning Electron Microscopy instrument (Zeiss 10 kV field). Elemental analysis of the composites was also carried out by energy dispersive spectrometry (EDS, Shimadzu), while the interfacial interaction within the synthesized composites were obtained via High-resolution transmission electron microscopy (JEOL TEM), along with the selected area electron diffraction (SAED) pattern. The FTIR of the composites were measured on Perkin Elmer Series 100 Spectrum to determine the functional characteristics of the composites.

RESULT AND DISCUSSION

Structural Analysis

As shown in Figure 1, the principal diffraction peaks are at 2θ degrees 26.54, 34.02, 38.03, 51.72, 54.50, 65.88, and 78.54 corresponding to (110), (101), (200), (211), (002), (301), and (202) crystal planes which is compatible with the creation of pure cassiterite SnO_2 crystallite free of impurities. The results illustrated above suggests that there is a gradual increase in peak intensities corresponding to the loading of varying quantities of graphene oxide (GO). Furthermore, the characteristic peaks of GO are absent from the GO-SnO_2 composites due to the modest proportion of GO in these materials. Ultimately, the lack of additional peaks in the nanocomposite demonstrated that the photocatalysts were completely free of contaminants in their prepared state.

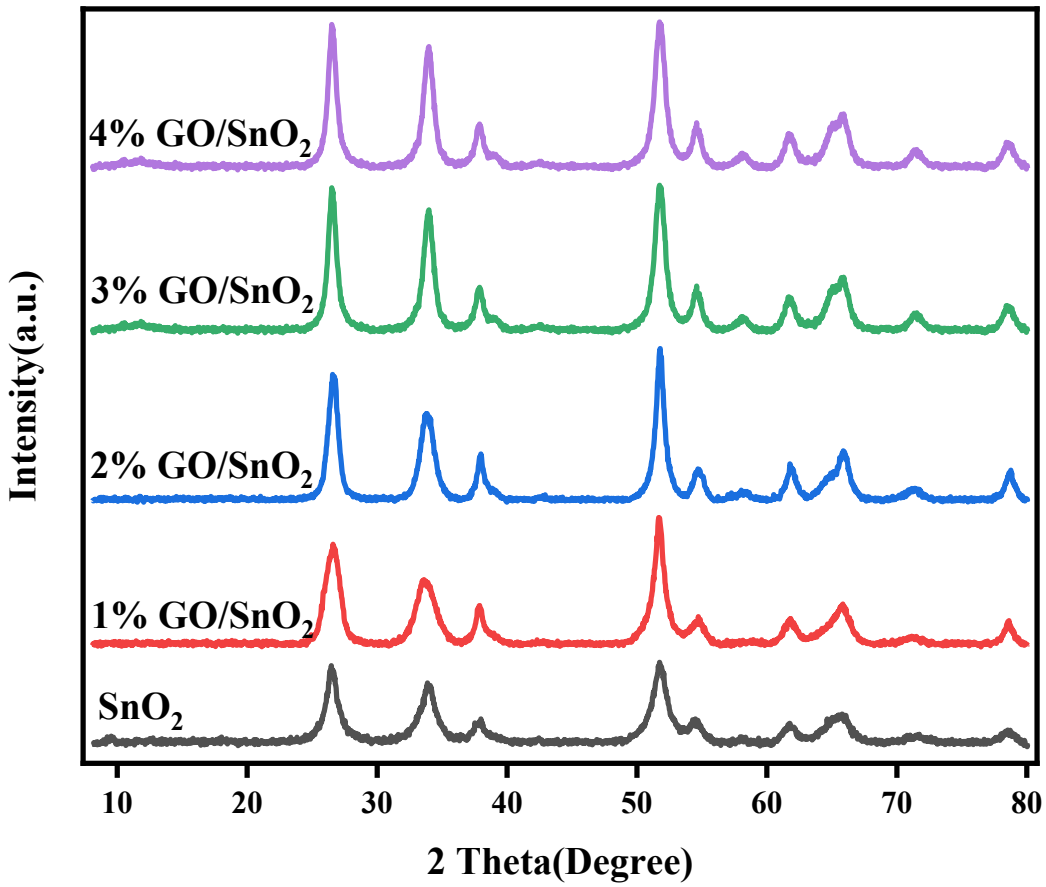

Figure 1: XRD patterns of SnO_2 and its respective GO-SnO_2 composites.

The FTIR spectral of the prepared nanoparticles as displayed in Figure 2 shows that there are presence of several peaks in the pure SnO_2 nanoparticles, which correspond to Sn–O and O–Sn–O, respectively, at around 528, and 668 cm^{-1}. O–H, CO_2, and C—O functionality can be attributed to the peaks at 3448, 1835, and 1724 cm^{-1}, respectively. Meanwhile, other functional groups with only slight differences are visible when different weight percentages of GO are incorporated into SnO_2.

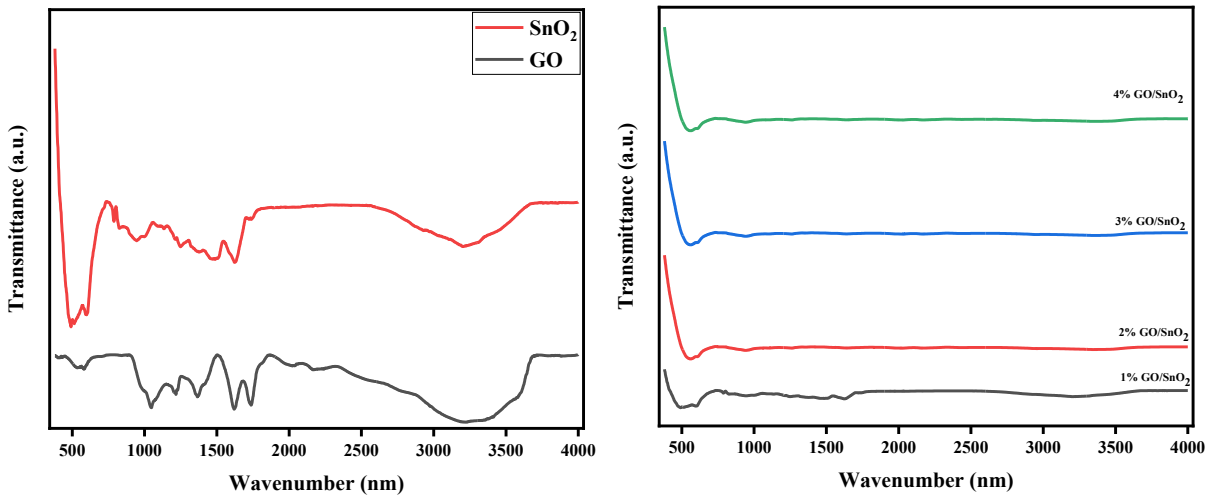

Figure 2: FTIR spectra of the synthesized composites

MORPHOLOGICAL ANALYSIS

The morphological evaluation of the prepared samples were done using the SEM analyzer, as show in Figure 3a, is evident that graphene oxide (GO) has a sheet-like structure, which is a sign of a well synthesized material while the SnO_2 particles have a surface morphology that is almost uniform, and they appear to be in a mixed condition that includes both parted and agglomerated forms [21]. It is clear that tiny GO nanoparticles aggregate to form bigger clusters on the surface of SnO_2, a characteristic shared by all nanocomposite morphologies.

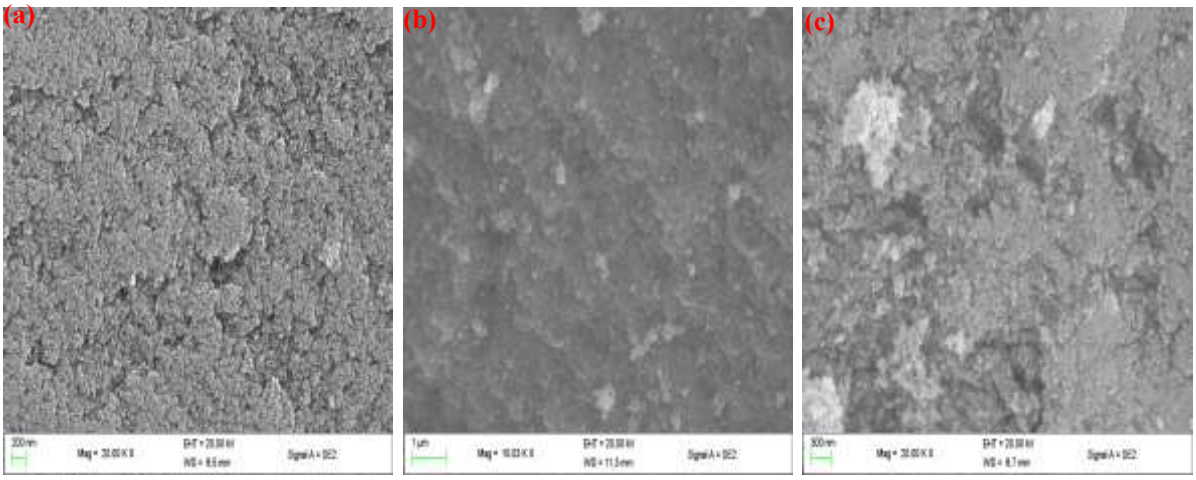

Figure 3: SEM image of synthesized (a) GO, (b) SnO_2 and GO/SnO_2 composites

The chemical composition of the nanoparticles is confirmed by the EDS of the produced GO-SnO_2 samples, which is also reported. The EDS spectra of the modified GO/SnO_2 showed the presence of the

following element Sn, C, N and O, with C and N having lower atomic percentages which could be as a result of the low weight percentages of GO used in the synthesis.

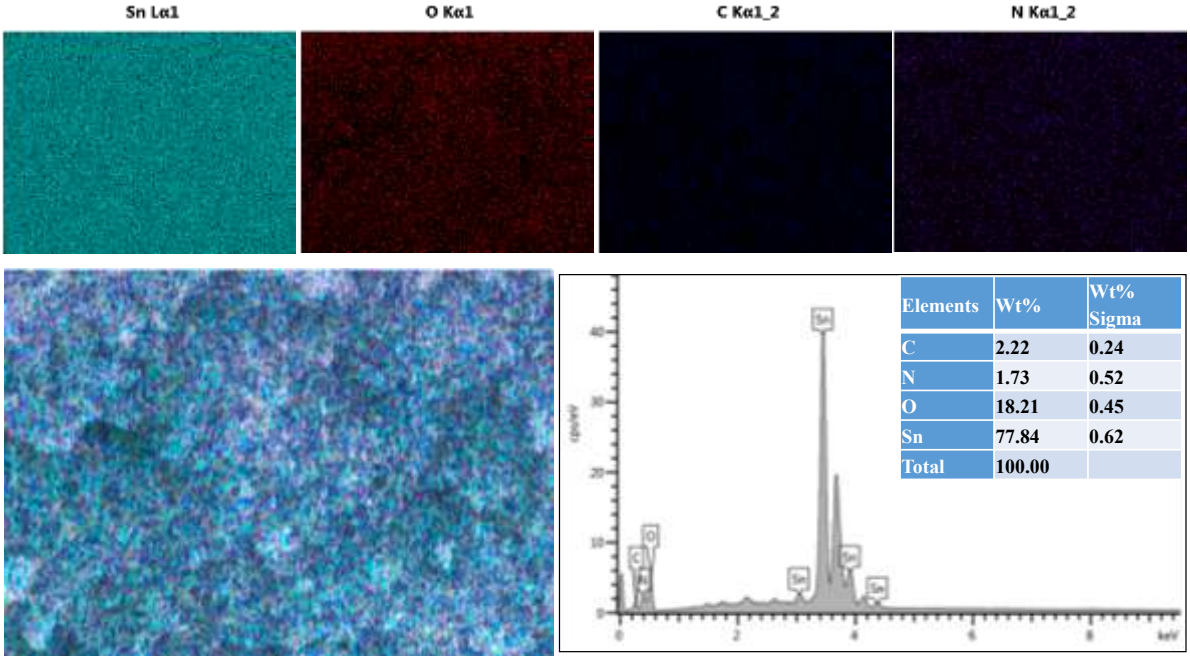

Figure 4: SEM-EDS elemental mapping and EDS spectrum of GO-SnO_2

The TEM pictures of the prepared nanoparticles reveals that the sheets that make up GO have a curly morphology, with the edges of the sheets somewhat folded and scrolled. The TEM image of SnO_2 nanoparticles depicts an agglomeration of almost tiny spherical particles. As illustrated in Figure 5(c), the GO-SnO_2 showed dispersion of GO on the composites of GO-SnO_2 which means the successful construction of heterojunctions between GO nanosheet and SnO_2 nanoparticles [19]. The SAED spectrum of the composites in Figure 5(d) shows that the crystallinity of the SnO_2 nanoparticle remains intact even with the inclusion of GO purposely due to the low quantity of GO in the composites.

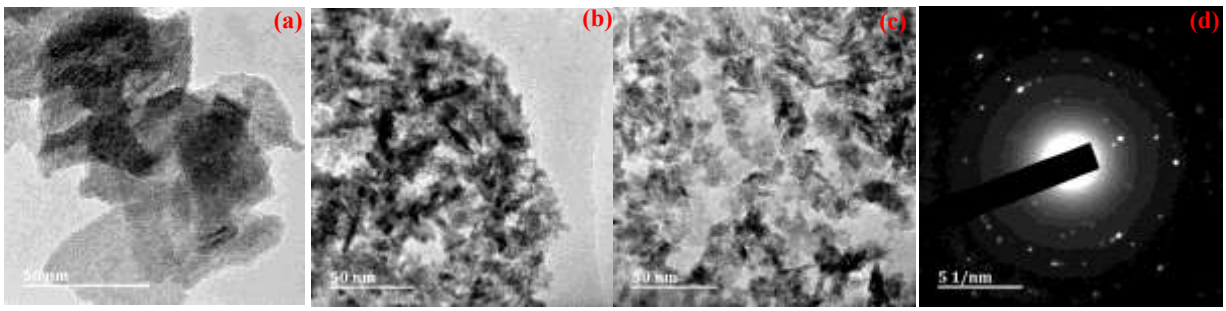

Figure 5: TEM images of (a) GO, (b) SnO_2, (c) GO-SnO_2 and (d) SAED spectrum of GO-SnO_2

The GO-SnO_2, SnO_2, and synthesized GO surface areas were measured utilizing the nitrogen adsorption and desorption isotherm of a BET analyzer. Adsorption-desorption profile followed type IV characteristic with type H3 hysteresis loop, indicating mesoporous structure development for all the synthesized composites. In comparison to SnO_2, the synthesized varying masses of the composite materials showed an increase in BET specific surface area. In particular, the addition of GO, which has a surface area of 1392.28 m^2/g, caused the surface area of SnO_2 to rise from 12.26 m^2/g to 39.37 m^2/g. The cross-sectional area of the pollutants and the adsorption surface area grew together, improving the composite's photocatalytic efficacy.

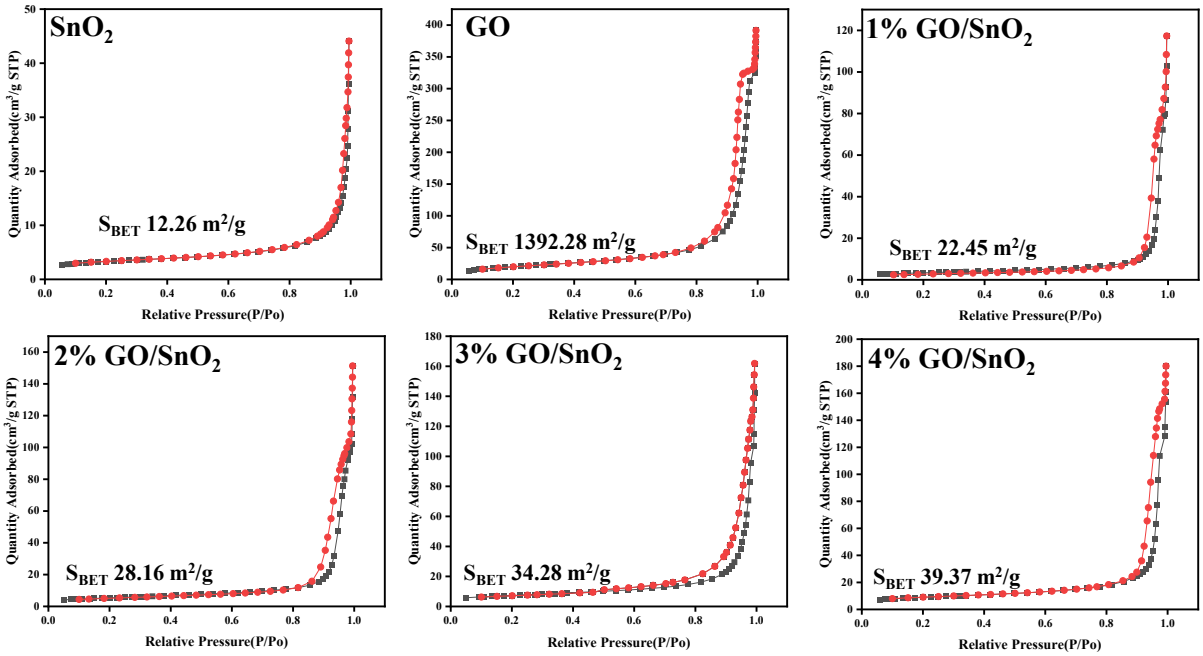

Figure 6: Nitrogen adsorption-desorption isotherms of the synthesized materials

In Figure 7a, the UV-vis absorption spectra shows that the optical absorption edges of SnO_2 nanoparticles are at about 410 nm, which cannot make full use of visible light while for the difference masses of GO/SnO_2 nanocomposites, the absorption shows a broad elevated background in the visible region with increasing content of GO nanosheet implying that the GO could optimize the optical absorption ability of GO/SnO_2 nanocomposites. This phenomenon indicates that more solar energy can be absorbed by the photocatalyst, which is beneficial for photocatalytic degradation of organic pollutants. Furthermore, in Figure 7b, the Eg (band gap) values of SnO_2 nanoparticles and the difference masses of GO/SnO_2 are 3.12, 2.75 and 2.62 eV, respectively. It is obvious that the optical band gap of GO/SnO_2 nanocomposites gradually decreased with the increasing amount of GO when compared to pristine SnO_2 nanoparticle.

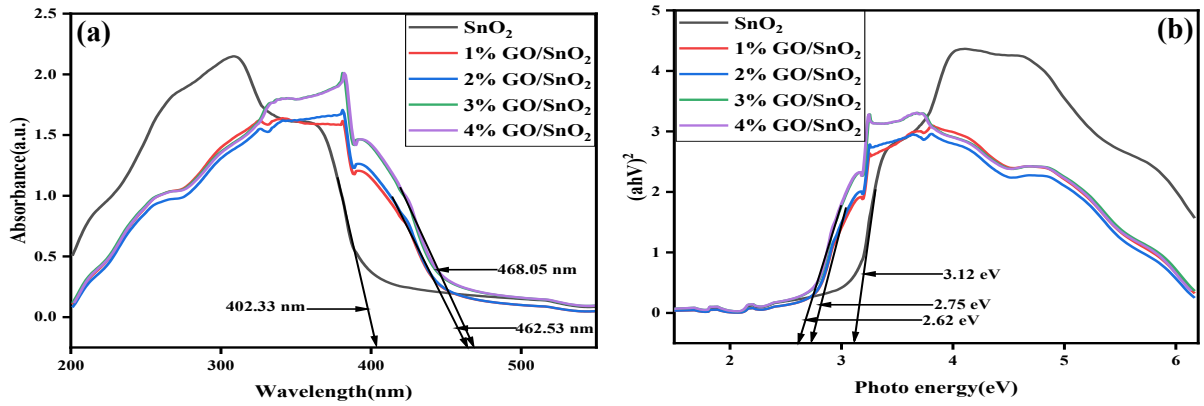

Figure 7: (a) UV–vis DRS spectrum and (b) Kubelka-Munk plot of the synthesized composite

Figure 8 shows the PL spectrum of the synthesized nanoparticles; it can be seen that the SnO_2 peak intensity is decreased by the GO nanosheet when GO serves as an electron sink. It can be seen that the PL spectral intensity of the different masses of the composites of GO/SnO_2 nanocomposites are all lower than that of pure SnO_2 nanoparticle, indicating that there is a formation junction between GO and SnO_2 which can facilitate photo-generated charge transfer. In addition, 3%GO/SnO_2 shows extremely low PL spectrum intensity, suggesting a noticeable improvement in the suppression of charge recombination. [16].

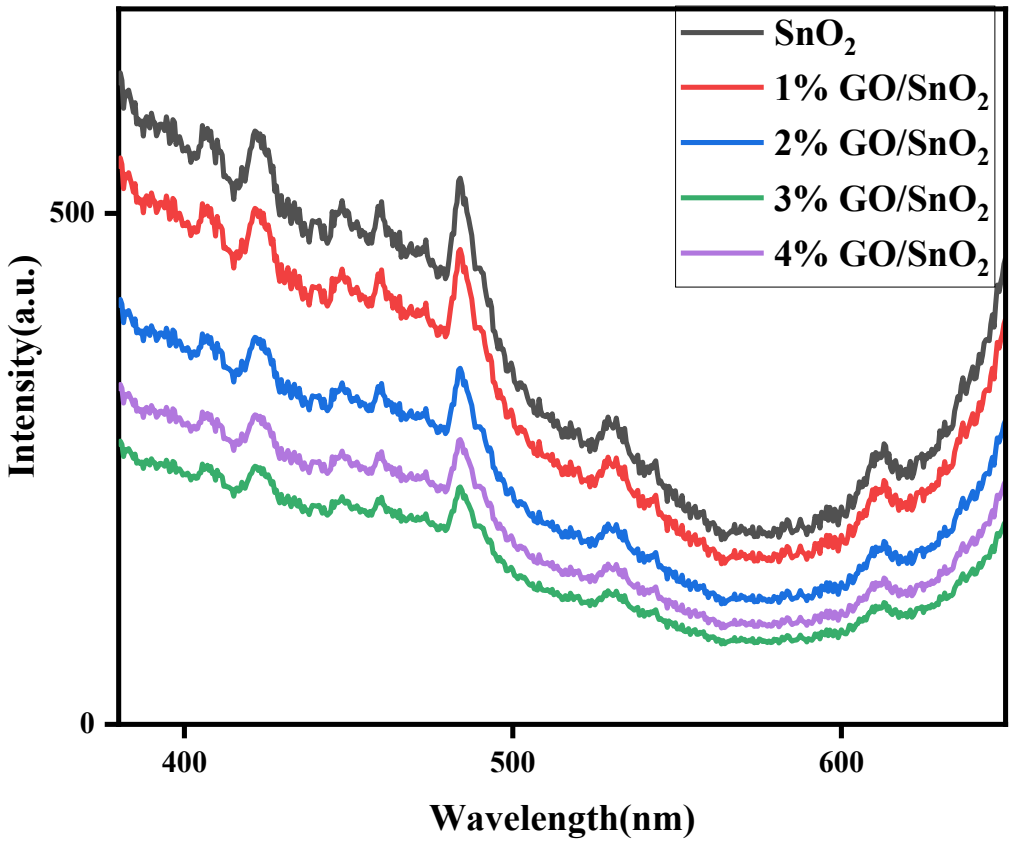

Figure 8: PL spectrum of SnO_2 and GO/SnO_2 composites

Photocatalytic Performance

Figure 9 the photocatalytic performance of SnO_2 and the varied masses (1, 2, 3 & 4) wt. % of GO/SnO_2 nanocomposites achieved degradation efficiencies of 44.70%, 75.18%, 86.97%, 93.42% and 90.01% respectively with methylene blue removal under visible light irradiation in 180 minutes. This indicates that the degradation rate improved with increasing GO content, with optimal performance being reached at 3% GO/SnO_2 weight percentage. Increase in GO content above this weight percentage decreased the amount of photocatalytic activity, probably because the GO aggregated within the SnO_2 nanosheet, reducing its active surface area and introducing recombination sites. Kinetic analyses were employed to compare the methylene blue degradation rate of the composites according to the logarithmic ratio of C_0 (initial concentration of the MB) and Ct (the concentration of the MB at the time of t), which the following relationship has carried:

$\ln C_0/Ct = k_{abs}t$

Where k_{abs} is the rate constant of the absorption. If the ln C_o/Ct vs.t plotting is drawn by matching the data with straight lines, then the slope of these lines will indicate the absorption rate of the samples. These results are presented in Figure 9b shows that the 3% GO/SnO_2 nanocomposites show the most excellent k(abs) which can be attributed to the synergetic effects of GO on SnO_2 [20].

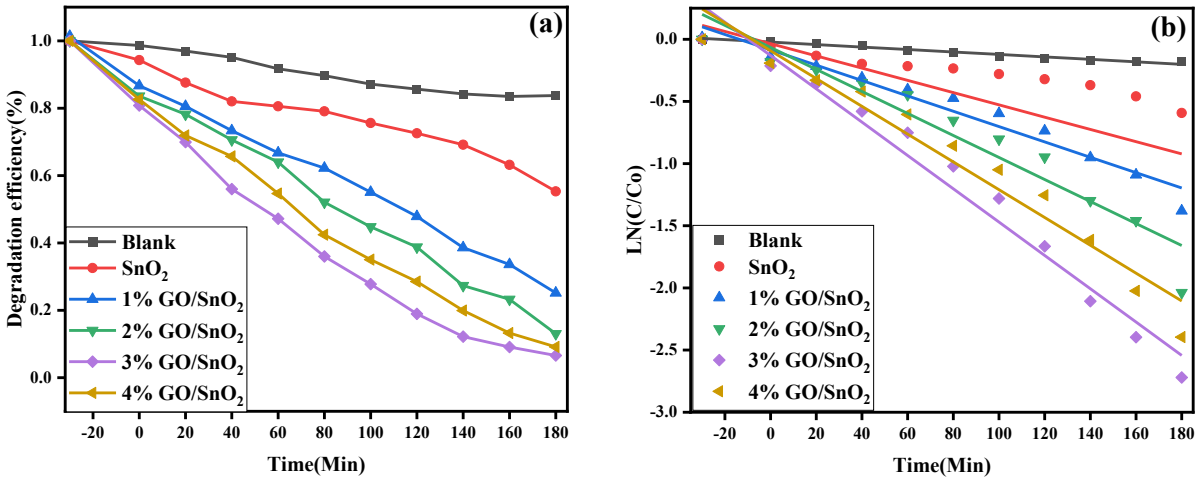

Figure 9: (a) Photocatalytic efficiency of SnO_2 and its corresponding composites for the degradation of methylene blue, (b) their kinetics plot.

Mechanisms Of Sno_2 Photocatalysts For The Degradation Of Mb

The mechanism of the photocatalytic reaction in the presence of SnO_2 photocatalysts comprises of a free radical reaction initiated by light irradiation [17]. When the energy of solar radiation exceeds the bandgap of SnO_2 (i.e., photon energy reaches or exceeds its bandgap energy), the surface of the photocatalyst becomes excited, and the electrons transit from the valence band (VB) to the conduction band (CB). In the CB, corresponding electron holes are derived in the VB at the same time, forming electron–hole pairs (i.e., generating electron (e) and hole (H^+) pairs). VB holes have strong oxidation reaction activity (1.0~3.5 V) because they lose electrons and act as reducing agents, and electrons in the conduction band have good reducibility 0.5~1.5 V when they undergo reduction. Under light irradiation, positive holes and electrons are generated in the VB (hv^+vb) and CB (e^-cb) of SnO_2 These holes can either form hydroxyl radicals or react directly with organic molecules which subsequently oxidize the organic molecules. The electrons can also react with organic compounds to produce reduction products [18].

The role of oxygen is important as it reacts with the photogenerated electrons. Organic compounds can then undergo oxidative degradation through their reactions with hydroxyl and peroxide radicals, VB holes, as well as reductive cleavage via reactions with electrons yielding various byproducts and finally mineral end-products.

$SnO_2 + hv \rightarrow SnO_2 + h^+ + e^-$-----(2)

$h^+ + H_2O \rightarrow OH^- + H^+$----------(3)

$SnO_2 (e^-) \rightarrow GO (e^-)$----------(4)

$O_2 + GO\ (e^-) \rightarrow O_2^-$----------(5)
$2H_2O + O_2^- \rightarrow 2OH^\cdot + 2OH$------(6)
$OH^\cdot + SnO_2 + MB \rightarrow CO_2 + H_2O + \ldots.$ (7)

CONCLUSION

This study examined the effect of graphene oxide (GO) on the photocatalytic performance of SnO_2 for the removal of methylene blue under visible light source irradiation. It was found that the functionalization of SnO_2 with GO enhanced its photocatalytic performance. It was also discovered that the electrical characteristics of the GO as an electron sink greatly influence the photocatalytic performance of the GO/SnO_2 in eliminating methylene blue in simulated water, which was one of the causes for the improvement in the properties of the synthesized SnO_2. Furthermore, it was noted that the addition of GO enhanced the surface area of SnO_2, increasing the formation of electron-hole pairs. Hence, this easy and affordable way to create a photocatalyst can be utilized to remove other organic contaminants from contaminated water since it works better at eliminating organic dyes like methylene blue.

REFERENCES

[1] Elshypany, R., Hanaa, S., Ahmad, H.M., Sadeek, A.S., Sharaa, S.I., Patrice, R., Amir, A.N. (2021) Elaboration of Fe_3O_4/ZnO nanocomposite with highly performance photocatalytic activity for degradation methylene blue under visible light irradiation. Environmental Technology Innovation 23, 101710

[2] Helmy, E. T., El Nemr, A., Mousa, M., Arafa, E., Eldafrawy, S. (2018). Photocatalytic degradation of organic dyes pollutants in the industrial textile wastewater by using synthesized TiO_2, C-doped TiO_2, S-doped TiO_2 and C, S co-doped TiO_2 nanoparticles. Journal of Water Environmental Nanotechnology, 3,116–127.

[3] Sanakousar, F., Vidyasagar, C., Jiménez-Pérez, V., Prakash, K. (2022). Recent progress on visible-light-driven metal and non-metal doped ZnO nanostructures for photocatalytic degradation of organic pollutants. Material Science Semiconductor Process, 140, 106390.

[4] Giahi, M. et al. Preparation of Mg-doped TiO2 nanoparticles for photocatalytic degradation of some organic pollutants. Stud. Univ. Babes-Bolyai Chem. 64, 7–18 (2019).

[5] Elaouni, A. et al. ZIF-8 metal organic framework materials as a superb platform for the removal and photocatalytic degradation of organic pollutants: A review. RSC Adv. 12, 31801–31817 (2022).

[6] Jiang, D. J., Tunmise, A. O., Yuanyuan, O., Noor, F. S., Song, W., Ailing, Z., Sanxi, L. (2021). A Review on Metal Ions Modified TiO_2 for Photocatalytic Degradation of Organic Pollutants. https://doi.org/10.3390/catal11091039

[7] Kayode, A.A., Olugbenga, S. B. (2015). Dye sequestration using agricultural wastes as adsorbents, Water Resource Industry, 12: 8–24, https://doi. org/10.1016/j.wri.09.002.

[8] Liu, Z. (2022). High efficiency of Ag0 decorated Cu_2MoO_4 nanoparticles for heterogeneous photocatalytic activation, bactericidal system, and detection of glucose from blood sample. Journal of Photochemical Photobiology B 236, 112571.

[9] Gusain, R., Gupta, K., Joshi, P. & Khatri, O. P. (2019). Adsorptive removal and photocatalytic degradation of organic pollutants using metal oxides and their composites: A comprehensive review. Advance College Interface. Science, 272, 102009.

[10] Mubarak, M. F., Selim, H., Elshypany, R. (2022). Hybrid magnetic core–shell TiO_2@ $CoFe_3O_4$ composite towards visible light-driven photodegradation of Methylene blue dye and the heavy metal adsorption: Isotherm and kinetic study. Journal of Environmental Health Science England 20, 265–280.

[11] Aniket, K., Lipeeka, R., Satish, K.A., Anurag, M., Rajendra, S.D., Priyabrat, D. (2016). An investigation into solar light driven enhanced photocatalytic properties of a graphene oxide-SnO_2-TiO_2 ternary nanocomposite. Journal of Royal society of chemistry advances Doi:10.1039/c6ra02067d

[12] Binaya, K.S., Rabindra, N.J., Madhusmita, S., Ravi, K., Das, A. (2021). Interface of GO with SnO_2 quantum dots as an efficient visible-light photocatalyst. Surface and nanoscience institute http://doi.org/10.1016/j.chemospere.130142

[13] Kent, F.C., Montreuil, K.R., Brookman, R.M., Sanderson, R., Dahn, J.R., Gagnon, G.A. (2011). Photocatalytic oxidation of DBP precursors using UV with suspended and fixed TiO2. Water Resources: 45: 6173-6180 https://doi.org/10.1016/j.watres.2011.09.013

[14] Heba, M.E., Amira, M.S., Rania, E., Hanaa, S. (2023). Efficient photocatalytic degradation of organic pollutants over TiO_2 nanoparticles modified with nitrogen and MoS_2 under visible light irradiation. Scientific Reports 13:8845 https://doi.org/10.1038/s41598-023-35265-7

[15] Dong, P., Wang, Y.,Guo, L., Liu, B., Xin, S., Zhang, J., Shi, Y., Zeng, W., Yin, S. (2012). A facile one-step solvothermal synthesis of graphene/rod-shaped TiO_2 nanocomposite and its improved photocatalytic activity, Nanoscale 4:4641-4649. https://doi.org/10.1039/c2nr31231j

[16] Khan, M.M., Ansari, S.A., Amal, M.I., Lee, J., Cho, M.H. (2013). Highly visible light active Ag@TiO_2 nanocomposites synthesized by electrochemically active biofilm: A novel biogenic approach, Nanoscale. 5:4427-4435. https://doi.org/10.1039/c3nr00613a

[17] Loh, K.P., Bao, Q., Ang, P.K., Yang, J. (2010). The chemistry of graphene, 2277–2289. https://doi.org/10.1039/b920539j.

[18] Lin, L., Yang, Y., Men, L., Wang, X., He, D., Chai, Y., Zhao, B., Ghoshroyb, S., Tang, Q. (2013). A highly efficient TiO_2@ZnO n–p–n heterojunction nanorod photocatalyst, Nanoscale. 5 588–593. https://doi.org/10.1039/c2nr33109h

[19] Lei, C. et al. Bio-photoelectrochemical degradation, and photocatalysis process by the fabrication of copper oxide/zinc cadmium sulfide heterojunction nanocomposites: Mechanism, microbial community and antifungal analysis. Chemosphere 308, 136375 (2022).

[20] Wang, Y., Zhang, M., Yu, H., Zuo, Y., Gao, J., He, G., Sun, Z. (2019). Facile fabrication of Ag/graphene oxide/TiO_2 nanorod array as a powerful substrate for photocatalytic degradation and surface-enhanced Raman scattering detection. Applied Catalysis B Environment 252, 174–186. [**Google Scholar**] [**CrossRef**

[21] Zhiqiang, W., Limin, W. (2019). Graphene oxide (GO)-doping SnO_2. flower-like structure to enhance photocatalytic activity. Fullerenes, Nanotubes and carbon Nanostructures, 27:5,387-394 https://doi.org/10.1080/1536383x.157